Available online at www.sciencedirect.com
ScienceDirect
Journal of Sound and Vibration 308 (2007) 579–590
JOURNAL OF SOUND AND VIBRATION
www.elsevier.com/locate/jsvi

Dynamic characteristics of a new damping element based on surface extension principle in nanopore

Takuzo Iwatsubo[a,*], Claudiu V. Suciu[b], Masayuki Ikenagao[c], Kazuhiko Yaguchio[d]

[a]Department of Mechanical System Engineering, Kansai university, Yamate 3-3-35, Suita, Osaka 5648680, Japan
[b]Department of Intelligent Machines, Fukuoka Institute of Technology, 3-30-1 Wajiro-Hogashi, Higashi-ku, Fukuoka 8110295, Japan
[c]Damping & Isolation Division, Oiles Corporation, Hamamatsucho Square 30-5, Hamamatsucho 1-chome, Minato-ku, Tokyo 1058584, Japan
[d]Team Mirai, Fuji Silysia Chemical Ltd., 1846, 2-chome, Kozoji-cho, Kasugai, Aichi 4870013, Japan

Accepted 20 June 2007
The peer review of this article was organised by the Guest Editor

Abstract

This paper presents a development of a new damping element which is used as a principle of surface extension in nanopore. The surface extension force of water in hydrophobic nanopore in pressurization process is different from that decompressurization process. This principle is applied to a damping element. The nanopore is constructed by silica gel. A silica gel ball of 100–200 μm ∅ has many nanopores of 7–20 nm ∅ in it. The coated spherical silica gel and water are inserted in a piston–cylinder unit in order to work as a damper. If compression force is added to the piston–cylinder unit (damper), water flows into the nanopore under balance of pressure and surface extension force. If this damper is decompressed, water moves out to the outlet of the pore. The surface extension forces for compression are larger than that of decompression. This difference in force of the surface extension produces a damping energy.

Size of the pore, performance of surface extension force, fatigue life of coated material and static characteristics of the damper have already been presented by our group. Hence dynamic characteristics are presented in this paper. Two types of dampers, single cylinder type and double cylinder type, are presented, and energy dissipations of these two dampers are investigated for frequency response and piston stroke.

Then the following conclusions are arrived at:

(1) Energy dissipation of the single cylinder-type damper is larger than that of the double cylinder-type damper.
(2) Amount of energy dissipation is almost constant, even if the input frequency is changed. This characteristic is different from the oil damper.
(3) Damping efficiency for unit volume is very high, so large energy can be dissipated by small size damper.
(4) Heat does not occur by the dissipation of energy. So characteristics of damping performance do not change by temperature.

*Corresponding author. Tel.: +81 6 6368 0855; fax: +81 6 6388 8785.
E-mail address: iwatsubo@ipcku.kansai-u.ac.jp (T. Iwatsubo).

0022-460X/$ - see front matter © 2007 Published by Elsevier Ltd.
doi:10.1016/j.jsv.2007.06.012

1. Introduction

Ability of fluids, flowing in narrow interstices, to dissipate the energy of shock and vibration is well known. The specialized machine element for this is called viscous damper [1,2]. The fluid flow can be Couette (Lanchester's absorber) or/and Poiseuille (hydro-pneumatic dampers, Squeeze film dampers, etc.). Hydraulic damper (HD) presented in Fig. 1(a) dissipates the mechanical energy by laminating the hydraulic oil to pass through calibrate holes. During a Poiseuille flow, the viscous force produces dissipation of the mechanical energy. External force F can be expressed as function of the piston velocity v and oil dynamic viscosity μ (Fig. 1(a)), where C and q are constants, which depend on the damper geometry. Since the oil viscosity is responsible for energy loss, this mechanism is called viscous dissipation [1,2]. Colloidal damper (CD), proposed by Eroshenko [3,4], is a device complementary to the HD, having a cylinder piston construction (Fig. 1(b)); no holes are machined on the piston; a mixture of hydrophobic porous matrix, e.g., modified silica gel, and its associated liquid, e.g., water, produce the colloidal suspension, which replaces the hydraulic oil. The porous matrix can from: silica gel, aero gel, ceramics, glass, zeolites, carbon (graphite, charcoal, fullerenes), aluminum oxide, etc. [3–8]. The working liquid can be [3–8]: water, aqueous solutions(e.g., water and antifreeze agent), mercury, melted metals (e.g.,1ead), melted alloys (e.g., wood alloy, eutectics), melted flux, melted salts, etc. From the ecological and economical point of view, the combination silica gel-aqueous solutions is convenient [8]. In the present work, only this type of colloidal suspension is considered. Silica gel matrix (Fig. 2) consists of porous particles of radius R, which is in the order of 1 μm–1 mm. The mesopores (Fig. 2) of variable radius γ occur as intersected nano-tubes, which follow complex directions in the case of labyrinth architecture. They occur as radial nano-tubes, parallely connected to a large hollow in the case of central cavity architecture. The whole, i.e., inner and outer, surface of the particles is hydrophobized with m-alkylchlorosilanes [7,8]. Due to its hydrophobic coating, the surface of the porous matrix is not wetted by water, i.e., the contact angle θ is higher than 90° (Fig. 2). At compression (Fig. 1(b)), water is forced to penetrate the porous matrix (Fig. 2). External pressure $p = 4F/(\pi D^2)$ works against the Laplace capillary pressure $-2\sigma \cos\theta/\gamma$ and the pressure of the gas (air and water vapors) trapped in the porous matrix (and this air trapped out the water):

$$p = -2\sigma \cos \theta/\gamma + p_g. \tag{1}$$

By analogy with mercury porosimetry (9), this mechanism was called water porosimetry [7]. CD concept is based on the observation that the compression and relaxation paths, in the graph of the pressure p versus stroke S, are not superposed and a hysteresis occurs. Thus, the same phenomenon, which lies at the basis of the water porosimetry, is employed here to dissipate the energy of vibration. Dissipated energy E is equal to the area of the hysteresis [8,9], i.e., it is equal to the work variation $\Delta W = -p\Delta V$ measured at the CD piston, where $\Delta V = \pi S D^2/4$ is the water volume variation. Introducing external pressure from Eq. (1) in the expression of

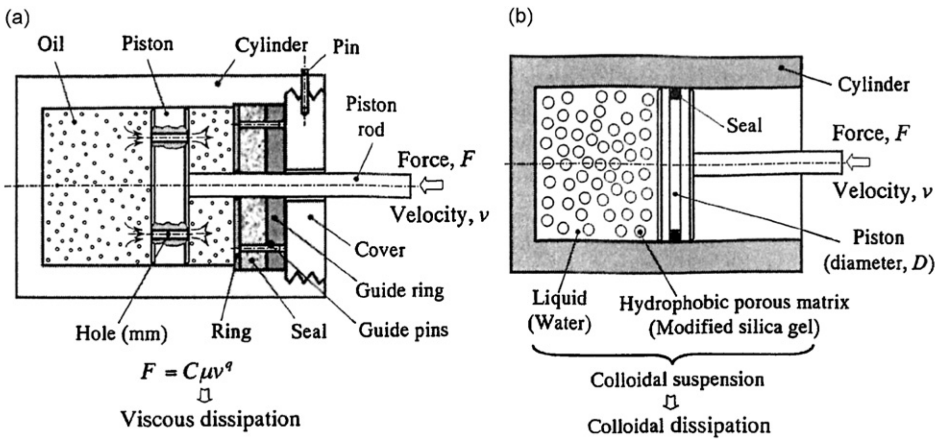

Fig. 1. Schematic view of hydraulic damper (HD) (a) and colloidal damper (CD) (b).

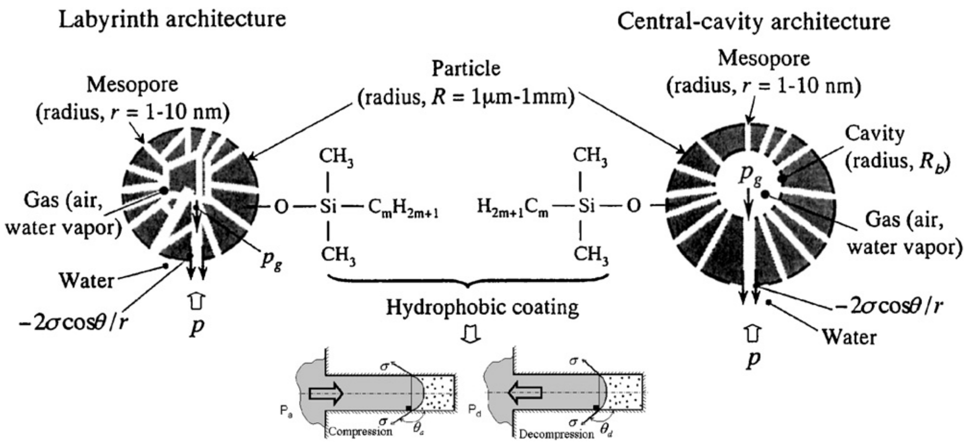

Fig. 2. Water penetration into a hydrophobic matrix of mesoporous silica gel.

work ΔW, and considering the relation between surface and volume variation $\Delta\Omega = 2\Delta V/\gamma$, one finds

$$\Delta W = \sigma \cos\theta \, \Delta\Omega - p_g \Delta V. \tag{2}$$

Since the gas pressure is negligible [8], CD occurs as a system able to transform the volume work ΔW into the interfacial work $\sigma \cos\theta \, \Delta\Omega$ of a solid–liquid–gas boundary. It was proved [8] that colloidal dissipation occurs due to the contact angle hysteresis on a rough and chemically heterogeneous surface. In compression, i.e., water adsorption, when the solid–liquid contact area increases ($\Delta\Omega > 0$), the contact angle is θ_a; at relaxation, i.e., water desorption, when the solid–liquid contact area decreases ($\Delta\Omega > 0$) the contact angle becomes θ_b. The difference $\theta_a - \theta_d$ might be of several tens of degrees, depending on the surface roughness and chemical inhomogeneities [10]. Figs. 1 and 2 illustrate that both HD and CD dissipate the mechanical energy by forcing the working fluid to pass through narrow holes. The difference between them is the size of the holes, which is in the order of millimeters for HD and in the nanometers for CD. As pointed out in Refs. [3–5,8,9,14,15], compared with HD, CD behaves unusually and displays several advantages: it is able to absorb large amount of mechanical energy, without heating; the CD dissipated energy does not depending by the piston velocity, and the CD efficiency is 2–3 times higher. Due to these important advantages, CD might replace HD in some applications such as dampers, vehicle suspensions, seismic dampers, buffers, engines supports, various antivibration protections. CD can be regarded as a novel application of Nanotechnology in the field of Mechanical Engineering. Nanotechnological aspects are connected to manufacture of silica gel with proper architecture and hydrophobic coating [7,8].

In our test, static characteristics of CD were investigated for silica gels coated with various kinds of coatings [11]. It is known for the static test that the dissipated energy of the nth hysteresis is reduced from the first hysteresis energy, but CD cycle is reproducible by quantity of silica gel, which is changed by pore in silica gel and loading pressure, etc. [12]. For the dynamic test CD maximum efficiency is 2–3 times higher than hydraulic damper maximum efficiency when bore of the cylinder is same. CD dissipated energy is almost constant with the piston speed augmentation and so on [12].

In this paper, influences of hydrophobic coating of silica gel, mesopore radius, loading pressure, loading frequency and stroke of the piston are investigated by an experimental method to realize the CD in practical use.

2. Experiment

2.1. Dynamic test ring

Fig. 3 shows an original design solution (from a practical point of view) of the single CD dynamic test rig. Fig. 4 shows the measurement equipment. Colloidal suspension supplies the test chamber, which is located inside the high-pressure cylinder. Design of the high-pressure cylinder (Fig. 3) is similar for the dynamic and

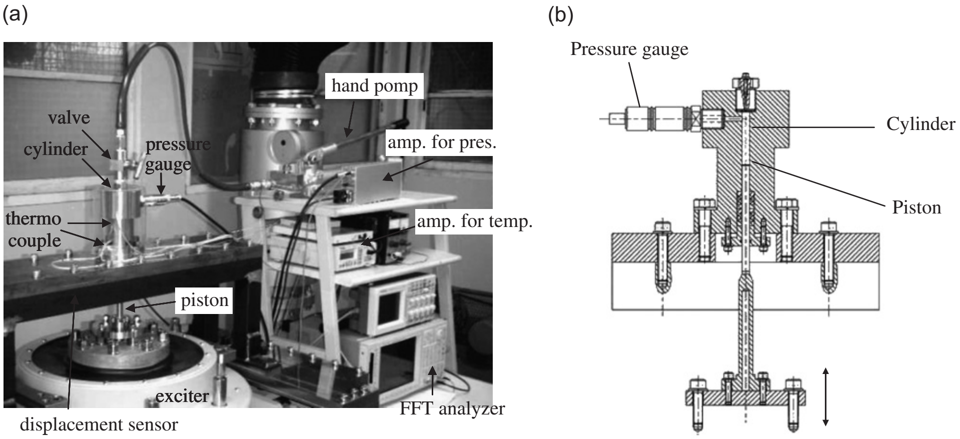

Fig. 3. Experimental apparatus: (a) overview of experimental apparatus and (b) detail of piston–cylinder unit.

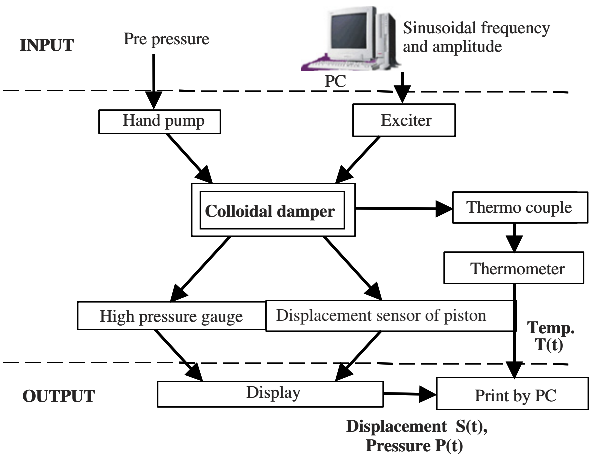

Fig. 4. Measuring systems.

static test rigs[2,4,6,7,13]. Piston of diameter $D = 8$ mm, thread plugs and high-pressure gauge close the test chamber. Copper gaskets, O ring and V packing are used to seal the experimental chamber, in which maximum pressure of 60 MPa can be created. A high-power vibration produces the dynamic load, which acts directly on the piston. Maximum force provided by vibrator is $F_{\max} = 9800$ N; the maximum stroke $S_{\max} = 51$ mm (peak–peak) and the maximum speed provided by vibrator $v_{\max} = 1$ m/s, i.e., 100 times higher than in static experiments [2,13].

This speed exceeds the critical velocity, which is on order of 20–200 mm/s [2,13]. Consequently one expects a quasi-adiabatic cycle of CD. Frequency range provided by vibrator is 2–2500 Hz, but one performs experiments in the range 2–40 Hz, since at higher frequencies, the amplitude of vibration is too small. One recalls here that CD becomes effective if the stroke is on order of several millimeters [2,4,6,7,13]. However, the frequency interval is selected according to specific applications: in the case of vehicle suspensions the frequency range is 0–40 Hz (e.g., the peak for the bullet train suspension is around 5 Hz); in the case of seismic dampers the frequency range is 0–20 Hz (the first peak occurs at 2–5 Hz and the second one at 8–11 Hz).We carried out dynamic measurements of the pressure p (high-pressure gauge), stroke S (displacement sensor) and temperature T (digital thermometer). Eliminating time t between pressure and stroke, the single CD dynamic hysteresis is found as a function $p = p\ (S)$. For different values of the frequency f, INPUT chain represents

Table 1
Coating of test material

Trade name	Sign of trade name	Coating materials	End capping	Mean pore diameter (nm)
SMB70-20-MT-C4	MT-C4	M, C4	With	7
SMB70-20-MT-C8	MT-C8	M, C8	With	7
SMB70-20-MT-C18	MT-C18	M, C18	With	7
SMB7020-DT-C8	DT-C8	D, C8	With	7
Fluorine coat-7	F7-17	F17	Without	7
Fluorine coat-10	F10-17	F17	Without	10

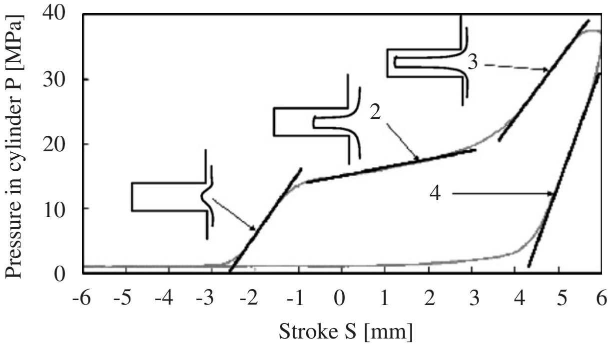

Fig. 5. Hysteresis curve and state of water in the pore.

a vibration testing system, consisting of computer, equipped with software for sinusoidal excitation; controller, which transmits the signal from computer to vibrator power source, and vibrator.

2.2. Materials

One observes that the hydrophobic porous silica, gel matrix, suitable for CD is actually used in the modern high-performance liquid chromatography [8,13]. Hydrophobic coating of silica gel (Fig. 2) was performed with short linear chains of alkylsilanes. Table 1 illustrates the main characteristics of the studied porous materials.

3. Dynamic characteristics of colloidal damper

It is known from previous investigation [16] that even if the working fluid is water without silica gel, damping force manifests by compressibility of water, V, the packing-piston deflection and O, the ring-piston deflection and this force depends on the loading frequency. This force is included in the test result of the colloidal damper.

Next, Fig. 5 shows the relation between hysteresis curve and water in the pore of the silica gel, in which the first part of the cycle is the beginning of entrance of the water in the pore, the second part is movement of water in the pore, the third is saturation of water in the pore and the fourth cycle is the return of the water by surface extension force due to relaxation of pressure.

3.1. Characteristics of single colloidal damper

Fig. 6 shows the typical hysteresis curve of colloidal damper, in which displacement of piston (i.e. effect of pre-pressure) and loading frequency are fixed. Upper and lower curves of the hysteresis show compression and relaxation cycles, respectively. So the cycle rotates clock wise. The area of these cycles gives the dissipative energy of the colloidal damper. The numbers in the figure show stroke of the piston. It is known from the

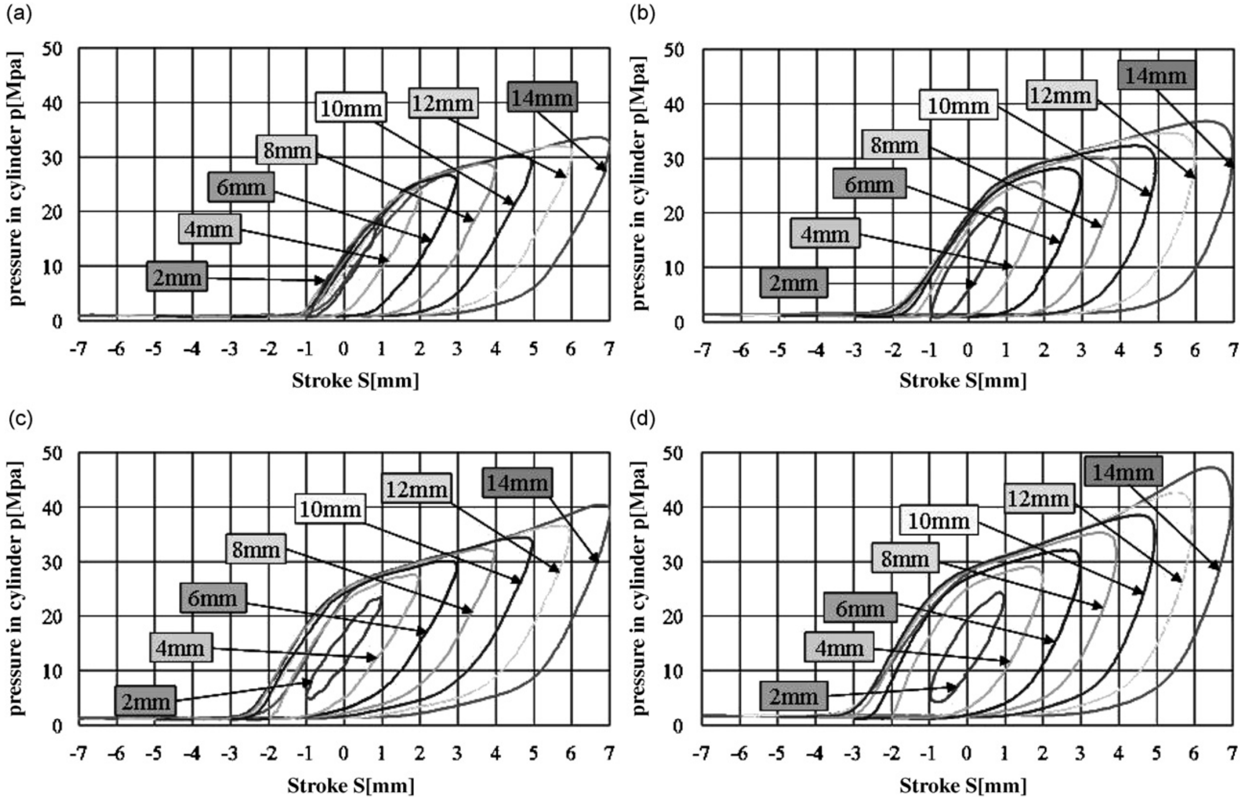

Fig. 6. Hysteresis curve of colloidal damper for SMB70-20-MT-C8: (a) pre-pressure: 8 MPa, frequency: 5 Hz; (b) pre-pressure: 8 MPa, frequency: 10 Hz; (c) pre-pressure: 12 MPa, frequency: 5 Hz; and (d) pre-pressure: 12 MPa, frequency: 10 Hz.

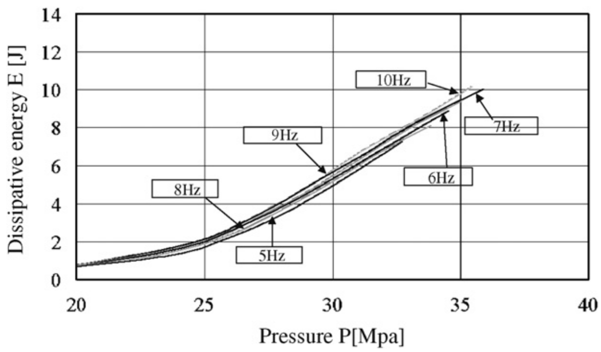

Fig. 7. Relation between cylinder pressure and dissipative energy (pre-pressure = 8 MPa, SMB70-20-MT-C8).

figure that dead zone exists in each cycle and these zones depend on the pre-pressure in the cylinder. Maximum pressure in the cylinder and area of hysteresis are increased as loading frequency increases.

Fig. 7 shows the relation between cylinder pressure (working pressure) and dissipative energy. As the pressure is increased, the dissipative energy increased. In the case of hydraulic damper, the dissipative energy depends on piston velocity, but in the colloidal damper, it depends on the maximum pressure of the cylinder. As it is clear from Fig. 5, that limit of maximum pressure in colloidal damper exists and it is determined by the pore diameter and the kind of coating, because the surface extension is decided by these values.

Fig. 8 shows the relation between cylinder pressure and efficiency of the damper, where the efficiency η is defined as the ratio of the area of hysteresis cycle to the area under the part of the upper hysteresis curve. The

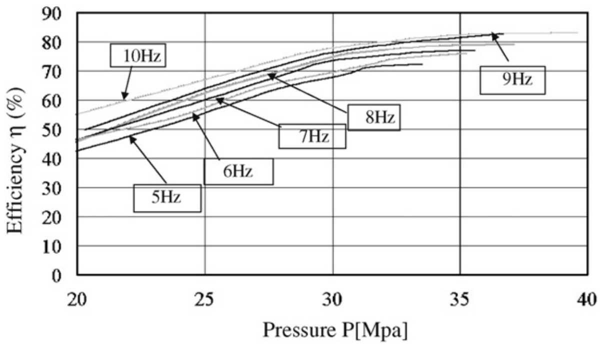

Fig. 8. Relation between cylinder pressure and efficiency (pre-pressure = 8 MPa, SMB70-20-MT-C8).

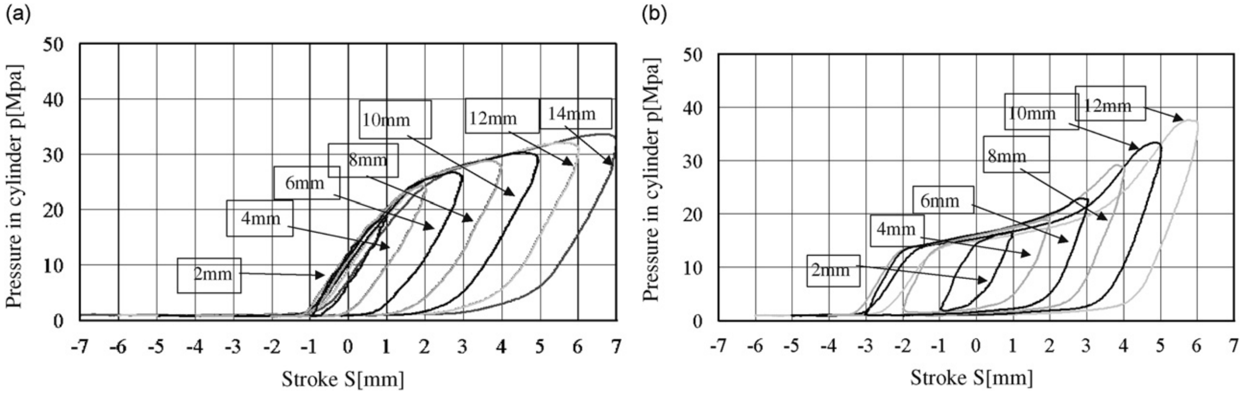

Fig. 9. Hysteresis curve for fluorine coating (pre-pressure = 8 MPa, loading frequency = 5 Hz): (a) pore diameter 7 nm; and (b) pore diameter 10 nm.

efficiency increased with increase in cylinder pressure and loading frequency. These results are almost same as in the other cases.

Fig. 9 shows the effect of pore diameter for silica gel modified by linear chain of Si Cu H_{2n} $(CF_2)_m$ CF_3 (called Fluorine coating). The figure shows that pressure of the second part of the hysteresis cycle of 7 nm pore diameter is higher than that of the 10 nm pore diameter and the third part of hysteresis cycle occurs for the 10 nm pore diameter. This phenomenon occurs by the change of front curvature of the water in the pore as shown in Fig. 10. That is, if the pore diameter is small, the front curvature of the water becomes round and contact angle σ becomes large due to the effect of surface extension of the water.

Fig. 10 shows the typical hysteresis curves for various kinds of coating materials, in which the last two words indicate the trade name, as in Table 1. The result of Fluorine coating with 10 nm pore diameter is a different hysteresis cycle compared to the other ones as shown in Fig. 11. This is caused by the pore size. Also MTC18 is a slightly different from the other ones. This is because the inside real diameter becomes small due to the long length of carbon chain of coating material.

For the pressure 8 MPa and load frequency 5 Hz, Figs. 12 and 13 show the relation between pressure in cylinder and the dissipative energy and efficiency, respectively. It is clear from these figures that 7 nm $\varnothing$ silica gels have same tendency but 10 nm $\varnothing$ silica gel has different tendency. The best performance silica gel is DTC8, then MTC8, Fluorine coating, MTC4 and MTC18 follow, in that order. But in the other case of pre-pressure and frequency, MTC8 performs best. The 10 nm diameter Fluorine coating has a quite different tendency and the performance does not depend on the pressure. This tendency was similar to that in other test condition of the pre-pressure and the load frequency. This tendency can be guessed by the pore diameter in the silica gel and the number of carbons chain of the coating material. From this result, number of carbon 8 is the

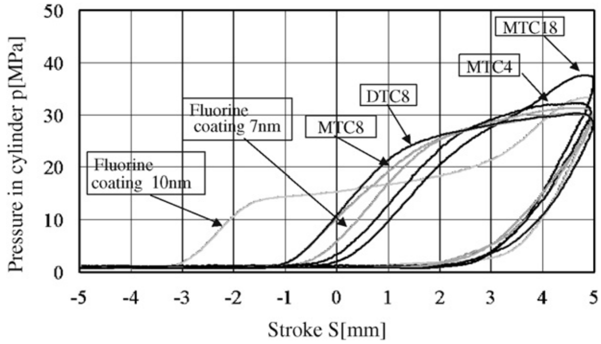

Fig. 10. Hysteresis curve for coating material and pore diameter (pre-pressure = 8 MPa, loading frequency = 5 Hz).

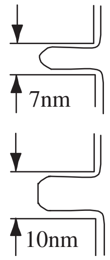

Fig. 11. Configuration of water in a pore.

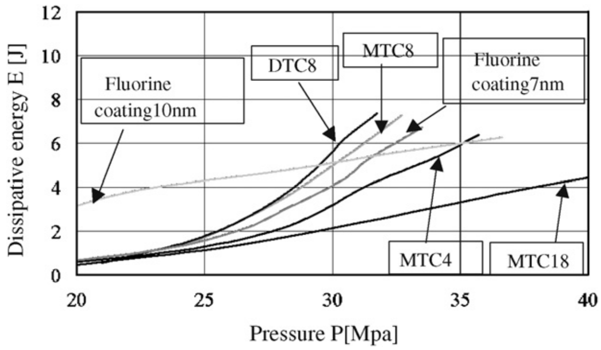

Fig. 12. Effect of coating material and pore diameter on the dissipative energy (pre-pressure = 8 MPa, frequency = 5 Hz).

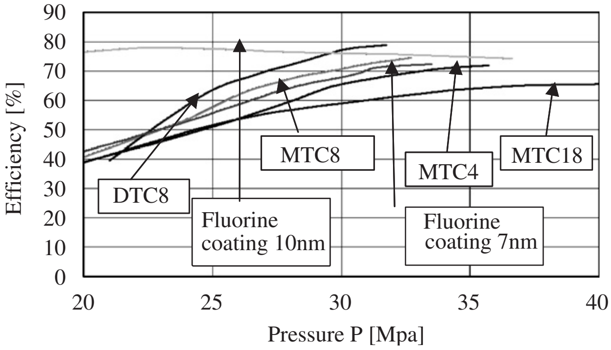

Fig. 13. Effect of coating material and pore diameter on the efficiency (pre-pressure = 8 MPa, frequency = 5 Hz).

best coating material for 7 nm pore silica gel. With regard to the load frequency, the dissipative energy and the efficiency become large as the load frequency increases.

Fig. 14 shows the effect of the pre-pressure on the dissipative energy and the efficiency for the parameter of the pre-pressure. It is clear from these results that the dissipative energy and efficiency depend on the pre-pressure and the working stroke range also depends on the pre-pressure as it is clear from the hysteresis curve. So it is necessary to design a colloidal damper that the pre-pressure and the stroke of the piston could be estimated.

3.2. Characteristics of double colloidal damper

The single colloidal damper operates only in compression process, but damping force in push and pull processes is sometimes required as a vibration damper. The double colloidal damper is designed for this requirement. Mechanism of the double colloidal damper is shown in Fig. 15. In order to avoid the outflow of air from the pore of silica gel, pre-pressure is needed in each chamber. So pre-pressure is created in each chamber by hand pump.

Fig. 16(a) and (b) give the hysteresis curves of the double colloidal damper (a) for the case of pore diameter 7 nm, SMB70-20-MT-C8 and pre-pressure 4 MPa, and (b) for the case of pore diameter 10 nm, the fluorine coating and pre-pressure 4 MPa. It is clear from these results that there is a space between positive and negative part of the pressure in the hysteresis curve because the pre-pressure of both chamber did not occur

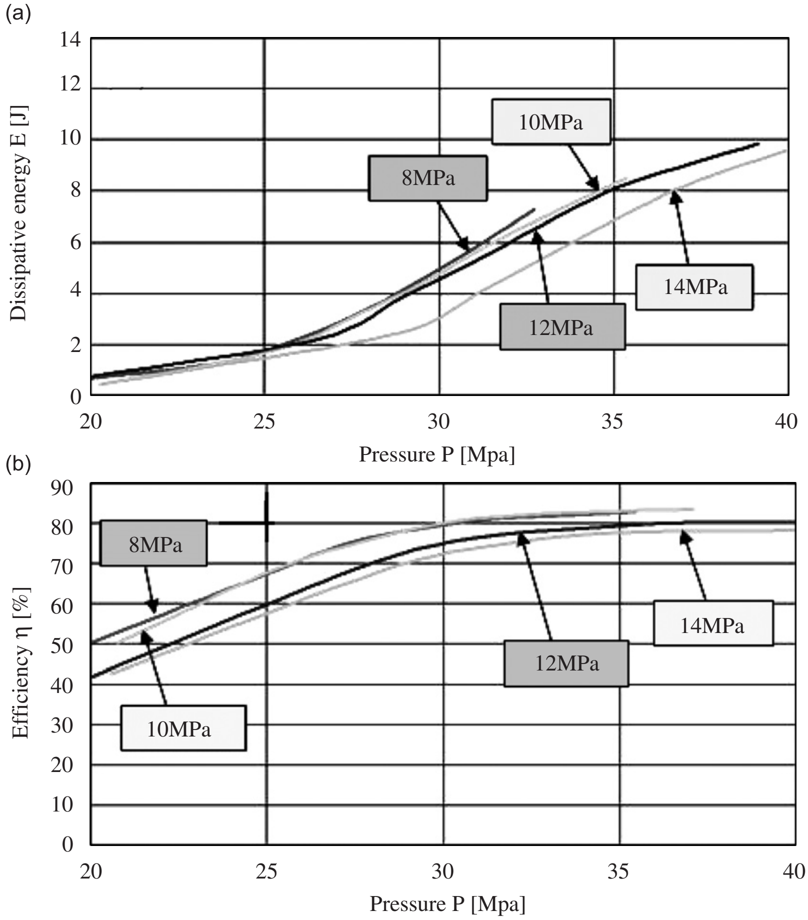

Fig. 14. Effect of pre-pressure on dissipative energy (a) and efficiency (b) for frequency 5 Hz.

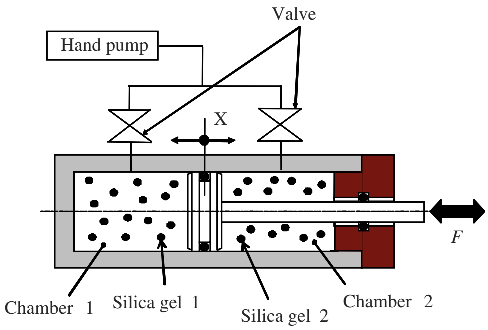

Fig. 15. Mechanism of double colloidal damper.

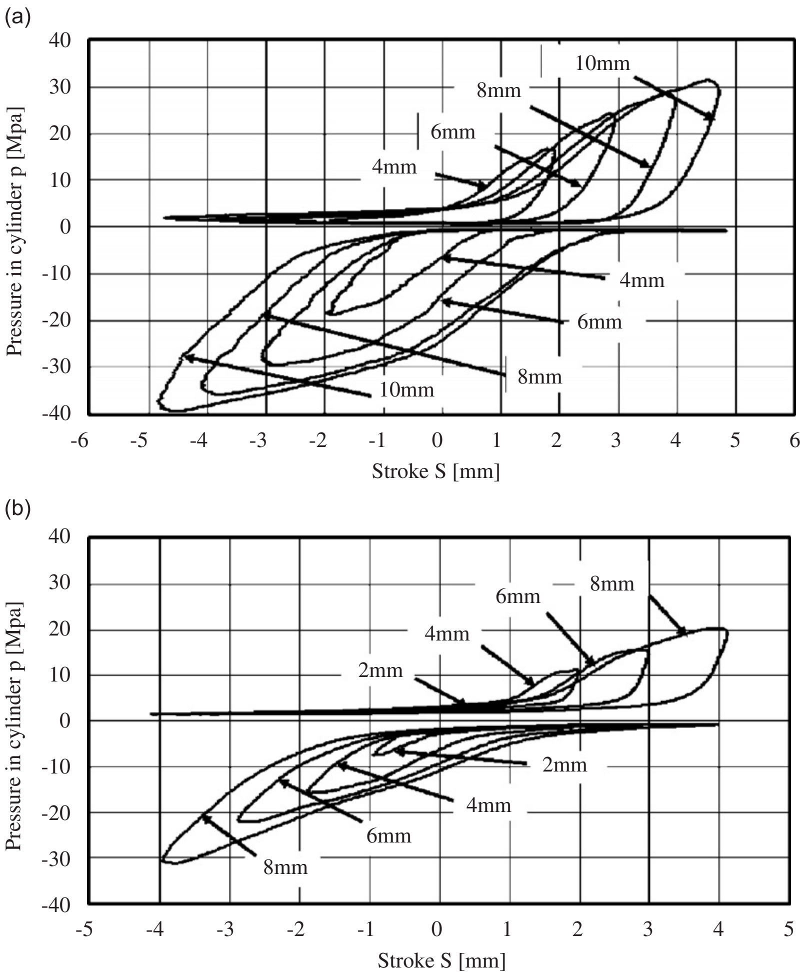

Fig. 16. Hysteresis curve of double colloidal damper: (a) pore diameter 7 nm, SMB70-20-MT-C8, pre-pressure = 4 MPa; and (b) pore diameter 10 nm, fluorine coating, pre-pressure = 4 MPa.

decompression as large as outflow of air from the pore. If the force of the piston rod is measured, the hysteresis curve will be continuous curve. Difference in hysteresis areas of positive and negative parts is due to the cross-sectional area of cylinder–piston system. Characteristics of upper or lower part of the hysteresis curves are almost the same as of the signal colloidal damper, but relation between the pre-pressure and the stroke should be considered in the design of colloidal damper, because if the stroke is too large and the pre-pressure is low in the operation, outflow of air from the pore will occur and operating condition will change.

Now let us compare the dissipative energy of the double colloidal damper with that of the single colloidal damper. If the single colloidal damper is used as a push and pull type damper by impressing the high pre-pressure and neutral, point of vibration moves to the center of the hysteresis, and dissipative energy of the single colloidal damper may be larger than that of colloidal damper.

4. Conclusion

This paper studied the dynamic characteristics of colloidal damper, in which six kinds of coating material are used, in order to use in actual applications. The effect of pre-pressure, working pressure, load frequency and stroke are changed as the parameter and dynamic characteristics are changed. Further the effect of number of carbon chain of coating, difference of combination between mono-chlorosilane (M) and di-chlorosilane (D) and difference of pore diameter for fluorine coating are investigated. The results are as follows:

(1) With regard to the parameter of working condition, pre-pressure governs the position of hysteresis center. If the pre-pressure becomes large, hysteresis center moves in the upward direction. The load pressure, which is almost proportional to the stroke, is sensitive to the area of hysteresis, i.e. dissipative energy and efficiency. The area of hysteresis becomes large with increase in the load pressure. The dissipative energy does not change so much with the increase in load frequency. A little increase of dissipative energy with the increase of frequency may be due to compressibility of water.
(2) With regard to the coating material, hysteresis area is changed by number of carbon chains. The largest hysteresis area was achieved by the number of carbon chain 8, so it is thought that this coating material is the best as a colloidal damper. As an addition to the silica-gel, di-chlorosilane was better than mono-chlorosilane from the view point of hysteresis area.
(3) With regard to the diameter of pore, characteristics was compared by fluorine coating and its chain was 17. In this case, if the pore diameter becomes large, the cylinder pressure becomes low for stroke, because the surface extension becomes low for large pore diameter.
(4) Energy dissipation of single colloidal damper may be larger than that of the double colloidal damper, if the single colloidal damper is used under high pre-pressure as large as the outflow of air from the pore of silica gel does not occur.

Acknowledgement

Authors would like to acknowledge the support by the Japanese Grant-in-Aid for Scientific Research No. 16360117-5001.

References

[1] N.P. Chironis, *Spring Design and Application*, McGraw-Hill, New York, 1961, pp. 204–242.
[2] C.M. Harris, C.E. Crede, *Shock Vibration Hand book*, McGraw-Hill, New York, 1982, pp. 1–418.
[3] V.A. Eroshenko, Heterogeneous energy accumulation or dissipation structure, methods for using such structure and associated apparatus, Patent 94/14856, 1994, pp. 1–20.
[4] V.A. Eroshenko, Damper with high dissipating power, Patent WO 01/55616 A1, 2001, pp. 1–44.
[5] R. De la Taille, Des Trous Noirs Dans un Amortisseur, *Science et Vie* (1995) 70–75 (in French).
[6] V.A. Eroshenko, R.C. Regis, M. Soulard, J. Patarin, Energetics: a New Field of Applications for H Chemical Society, Vol. 123(2), 2001, pp. 8129–8130.
[7] A.Y. Fadeev, V.A. Eroshenko, Study of penetration of water into hydrophobized porous silicas, *Journal of Colloid and Interface Science* 187 (1997) 275–282.
[8] C.V. Suciu, T. Iwatsubo, S. Deki, Investigation of a colloidal damper, *Journal of Colloid and Interface Science* 259 (1) (2003) 62–80.
[9] T. Iwatsubo, C.V. Suciu, S. Deki, Theoretical investigation of a colloidal damper, *Proceedings Asia-Pacific Vibration Conference*, Vol. 2, 2001, pp. 407–411.

[10] D.R. Lide, *Handbook of Chemistry and Physics*, CRC Press, Boca Raton, FL, 1999, pp. 1–523.
[11] C.V. Suciu, T. Iwatsubo, S. Deki, Novel principle of mechanical energy dissipation (part 1: static performance of colloidal damper), *JSME International Journal Series C* 47 (1) (2004) 180–188.
[12] C.V. Suciu, T. Iwatsubo, S. Deki, Novel principle of mechanical energy dissipation (part 2: dynamic performance of colloidal damper), *JSME International Journal Series C* 47 (1) (2004) 189–198.
[13] S.J. Gregg, K.S.W. Sing, *Adsorption, Surface Area and Porosity*, Academic Press, New York, 1982, pp. 1–352.
[14] V.A. Eroshenko, Effect of heat exchange on filling of lyophobic pores and capillaries with liquid, *Colloid Journal* 49 (5) (1995) 875–880.
[15] V.A. Eroshenko, The role of thermodynamic and cosmic factors in evolution of coral reefs, *Mendeleev Chemical Journal* 39 (2) (1995) 84–102.
[16] C.V. Suciu, T. Iwatsubo, K. Yaguchi, M. Ikenaga, Study of the contact line movement past a solid surface from hydrophobized silica gel, *Journal of Colloid and Interface Science* 0 (2004) 1–19.